Monte Carlo simulation of the irreversible growth of magnetic thin films

Julián Candia[a] and Ezequiel V. Albano[b]
Instituto de Investigaciones Fisicoquímicas Teóricas y Aplicadas, (INIFTA), CONICET, UNLP, Sucursal 4, Casilla de Correo 16, 1900 La Plata, Argentina

(Received 26 March 2001; accepted for publication 24 August 2001)

The growth of magnetic films with ferromagnetic interactions between nearest-neighbor spins is studied in $(d+1)$-dimensional rectangular geometries for $d=1,2$. Magnetic films are grown irreversibly by adding spins at the boundaries of the growing interface. The orientation of the added spins depends on both the energetic interaction with already deposited spins and the temperature through a Boltzmann factor. At low temperatures thin films, of thickness L, are constituted by a sequence of well ordered magnetic domains. Spins belonging to each domain, of average length $l_D \gg L$, have mostly the same orientation, but consecutive domains have opposite magnetization. This kind of ''spontaneous magnetization reversal'' during the growth process has a short characteristic length l_R, such that $l_D \gg l_R \sim L$. At higher temperatures, a transition between ordered and disordered states is also observed. The emerging behavior is compared to that of the equilibrium Ising model. © *2001 American Institute of Physics.* [DOI: 10.1063/1.1412841]

I. INTRODUCTION

The preparation and characterization of magnetic nanowires and films is of great interest for the development of advanced microelectronic devices. Therefore, the study of the behavior of magnetic materials in confined geometries, e.g., thin films, has attracted both experimental[1–7] and theoretical[8–12] attention. From the theoretical point of view, most of the work has been devoted to the study of equilibrium properties of thin magnetic films.[8–12] In contrast, the aim of this work is to study the properties of thin magnetic film growth under far-from-equilibrium conditions. Within this context, a useful model for the study of the growth of magnetic materials is the so-called magnetic Eden model (MEM),[13] based on the well known Eden model.[14] The latter has become an archetypical growth model due to both its simplicity and interesting properties. Eden growth starts from a single particle called the seed. One then proceeds to add a new particle on a randomly chosen unoccupied site in the immediate neighborhood (the perimeter) of the seed. The growth process then continues by randomly adding new particles to the perimeter of the previously formed cluster. Although this simple rule leads to the growth of compact clusters filling the Euclidean space, the self-affinity that characterizes the behavior of the growing interface is of much interest.[15,16] The MEM, originally motivated by the study of the structural properties of magnetically textured materials, introduces an additional degree of freedom to the Eden model, namely the spin of the added particles.[13] More recently, the Eden growth of clusters of charged particles has also been studied.[17]

Considering the MEM with spins having two possible orientations (up and down), one can start the growth of the spin cluster from a single seed having a predetermined orientation, e.g., a spin up seed, placed at the center of the two-dimensional square lattice, whose sites are labeled by their rectangular coordinates i,j. Then, the MEM's growth process consists of adding further spins to the growing cluster taking into account the corresponding interaction energies. By analogy to the classical Ising model[18] one takes J as the coupling constant between nearest-neighbor (NN) spins S_{ij} and the energy E given by

$$E = -\frac{J}{2} \sum_{\langle ij,i'j' \rangle} S_{ij} S_{i'j'}, \tag{1}$$

where $\langle ij,i'j' \rangle$ means that the summation is taken over occupied NN sites. As we are concerned with spin $\frac{1}{2}$ particles, the spins can assume two values, namely $S_{ij} = \pm 1$.

It is worth mentioning that, while previous studies of the MEM were mainly devoted to determining the lacunarity exponent and the fractal dimension of the set of parallel oriented spins,[13] the aim of the present work is to study the growth of MEM films using extensive Monte Carlo simulations. In order to simulate thin film growth, our study is performed in confined (stripped) geometries which resemble recent experiments where the growth of quasi-one-dimensional strips of Fe on a Cu(111) vicinal surface[1] and Fe on a W(110) stepped substratum[7] have been performed. Also, in a related context, the study of the growth of metallic multilayers has shown a rich variety of new physical phenomena. In particular, the growth of magnetic layers of Ni and Co separated by a Cu spacer layer has recently been studied.[19]

Another goal of the present work is to compare the results obtained for the MEM with the well known behavior of the equilibrium Ising model,[18,20] an archetypical model in the study of phase transitions in equilibrium magnetic systems. The Ising Hamiltonian (**H**) is given by

[a]Present and permanent address: Departamento de Física, Facultad de Ciencias Exactas, Universidad Nacional de La Plata, C.C. 67, 1900 La Plata, Argentina.
[b]Author to whom correspondence should be addressed; electronic mail: ealbano@inifta.unlp.edu.ar

$$\mathbf{H} = -\frac{J}{2} \sum_{\langle ij,i'j' \rangle} S_{ij} S_{i'j'}, \tag{2}$$

where $\langle ij,i'j' \rangle$ means that the summation runs over all NN sites, $S_{ij} = \pm 1$, is the state of the spin at the site of coordinates i,j and J is the coupling constant ($J>0$ for the ferromagnetic case). It should be pointed out that, in spite of the fact that Eqs. (1) and (2) are similar, the MEM describes the irreversible growth of a magnetic material while the Ising model is suitable for the study of a magnetic system under equilibrium conditions, and hence these two models operate under extremely different conditions.

This article is organized as follows: in Sec. II we give details on the simulation method, Sec. III is devoted to the presentation and discussion of the results, while our conclusions are finally stated in Sec. IV.

II. DESCRIPTION OF THE MONTE CARLO SIMULATION METHOD

The MEM in $(1+1)$ dimensions is studied in the square lattice using a rectangular geometry $L \times M$ with $M \gg L$. The location of each site on the lattice is specified through its rectangular coordinates (i,j), $(1 \leqslant i \leqslant M,\ 1 \leqslant j \leqslant L)$. The starting seed for the growing cluster is a column of parallel oriented spins placed at $i=1$. As described in the foregoing section, the MEM growth occurs by selectively gluing spins at perimeter sites. It should be noted that previous studies of the MEM were performed using a single spin seed placed at the center of the sample.[13] In this way, previous simulations that followed this approach were restricted to rather modest cluster sizes, i.e., containing up to 8000 spins.[13] In contrast, the rectangular stripped geometry used in this work is suitable for the simulation of the growth of magnetic films and it also has significant technical advantages. Indeed, when the growing film interface is close to reach the limit of the sample ($i=M$) one simply computes the relevant properties of the irreversibly frozen film's bulk (in the region where the growing process has definitively stopped), and subsequently applies an algorithm such that the interface is shifted toward the lowest possible i coordinate (while, at the same time, the useless frozen bulk is erased). By repeatedly applying this procedure the growth process is not limited by the M value of the lattice. In the present work films having up to 10^9 spins have been typically grown. The described procedure can straightforwardly be extended to higher dimensions. In fact, we have also studied the MEM in $(2+1)$ dimensions employing a $L \times L \times M$ geometry $(M \gg L)$. Each site on the lattice is now identified through the rectangular coordinates (i,j,k), $(1 \leqslant i \leqslant M,\ 1 \leqslant j,k \leqslant L)$, and the starting seed for the growing film is taken to be a plane of $L \times L$ parallel oriented spins placed at $i=1$. The cutting-and-shifting algorithm is in this case also suitable in order to allow the growing film to acquire particles beyond the $i=M$ limit.

As already mentioned, the growth process of a MEM film consists of adding further spins to the growing film taking into account the corresponding interaction energies given by Eq. (1). A spin is added to the film with a probability proportional to the Boltzmann factor $\exp(-\Delta E/k_B T)$, where ΔE is the total energy change involved. It should be noted that at each step all sites of the growing perimeter are considered and the probabilities of adding up and down spins to them have to be evaluated. After proper normalization of the probabilities the growing site and the orientation of the spin are determined through a pseudorandom number generator. Throughout this work we set the Boltzmann constant equal to unity ($k_B \equiv 1$), we consider $J>0$ (i.e., the ferromagnetic case) and we take the absolute temperature T measured in units of J.

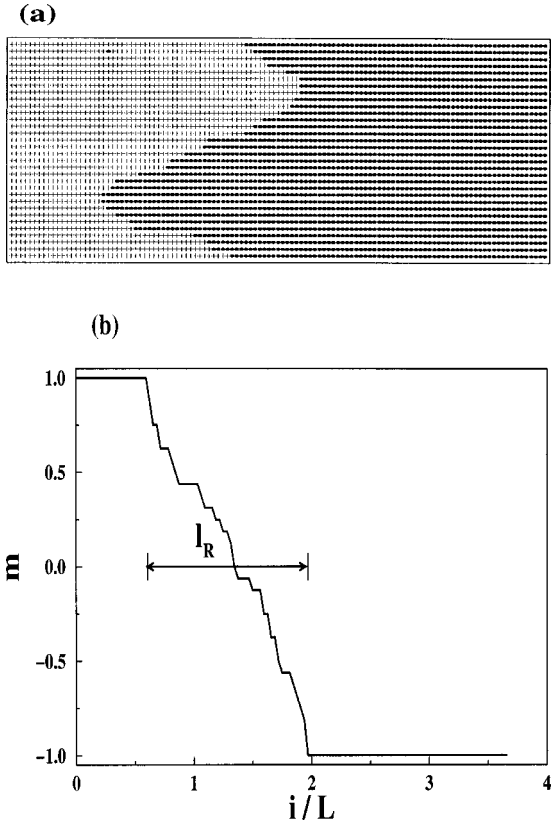

FIG. 1. Spontaneous magnetization reversal observed for $L=32$ and $T=0.26$ in the $(1+1)$-dimensional magnetic film. (a) Snapshot configuration that shows the collective orientation change: the left (right) domain is constituted by up (down) oriented spins. The snapshot corresponds to the bulk of the sample and the growing interface is not shown. (b) Magnetization profile associated to the upper configuration. The characteristic length for the occurrence of the magnetization reversal l_R is on the order of the lattice width, as marked in the figure.

III. RESULTS AND DISCUSSION

Magnetic Eden films grown on a stripped geometry of finite linear dimension L at sufficiently low temperatures show an intriguing behavior that we call spontaneous magnetization reversal. In fact, we have observed that long clusters are constituted by a sequence of well ordered magnetic domains of average length $l_D \gg L$. Figure 1(a) shows a snapshot configuration of the $(1+1)$-dimensional MEM where the phenomenon of spontaneous magnetization reversal can be recognized. Here the reversal occurring between a domain of spins up (on the left side) and another one constituted by spins down (on the right), as well as the interface between both domains, can be clearly observed. It should be noted that the well known phenomenon of field induced magneti-

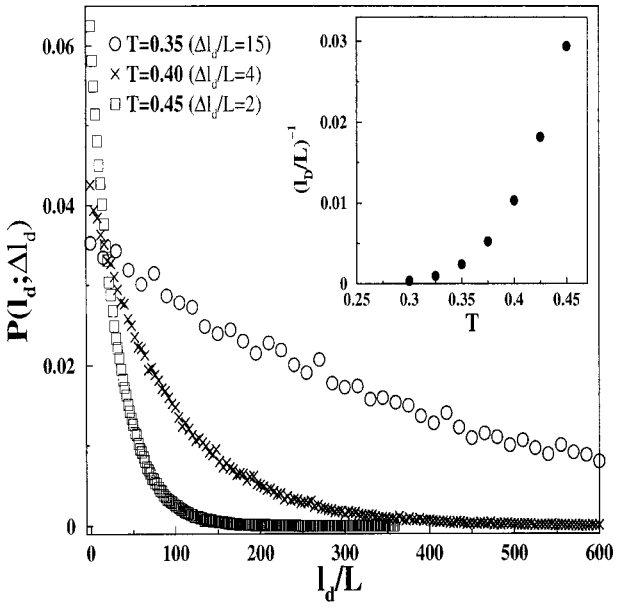

FIG. 2. Plots of $P(l_d;\Delta l_d)$ vs l_d/L for $L=16$ and different values of temperature and interval width, as indicated. The inset shows a plot of $(l_D/L)^{-1}$ vs T, also for a lattice of side $L=16$. As expected, increasingly long domains tend to show up at lower temperatures.

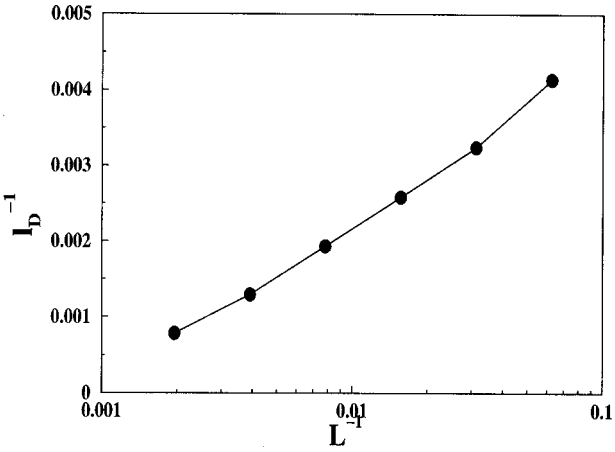

FIG. 3. Log–linear plot of l_D^{-1} vs L^{-1} for the temperature $T=0.5$ and lattice sizes in the range $16\leqslant L\leqslant 512$. The line is a guide to the eye, showing that the characteristic domain length diverges in the thermodynamic limit $(L\to\infty)$.

zation reversal in thin films[21,22] is quite different from the spontaneous reversal reported here. In the present study the reversal occurs during the growth process and in the absence of any applied magnetic field. The reported phenomenon is essentially due to the small size of the thin film and it becomes irrelevant in the thermodynamic limit. This theoretical prediction has not yet been observed experimentally. However, it will certainly be very interesting to design and carry out suitable experiments in order to observe this phenomenon.

Let l_R be the characteristic length for the occurrence of the spontaneous magnetization reversal. Since $l_R\sim L$, we then conclude that the phenomenon has two characteristic length scales, namely l_D and l_R, such that $l_D\gg l_R\sim L$. Figure 1(b) shows the magnetization profile that corresponds to the spontaneous magnetization reversal shown in Fig. 1(a), where

$$m(i,L,T)=\frac{1}{L}\sum_{j=1}^{L} S_{ij} \tag{3}$$

is the mean column magnetization at the distance $i-1$ from the seed, for a system of linear dimension L at temperature T. In Fig. 1(b) one can clearly observe how abruptly the magnetization drops from $m=+1$ to $m=-1$ within a characteristic length l_R of the order of L.

In order to investigate the dependence of the characteristic domain length l_D on L and T, let us define $P(l_d;\Delta l_d)$ as the probability for the formation of a domain of length between l_d and $l_d+\Delta l_d$. Clearly, the average domain length l_D mentioned above is the average value of l_d taken over a sufficiently long magnetic film (i.e., $l_D\equiv\langle l_d\rangle$ for $l_F\gg l_D$, where l_F is the film's total length). Figure 2 shows plots of $P(l_d;\Delta l_d)$ versus l_d/L for a fixed lattice size and different values of temperature. As expected, increasingly long domains tend to show up at lower temperatures. This behavior can be also observed in the plot of $(l_D/L)^{-1}$ versus T shown in the inset of Fig. 2. Figure 3 shows a log–linear plot of l_D^{-1} versus L^{-1} for a fixed temperature and lattice sizes in the range $16\leqslant L\leqslant 512$. This figure clearly shows that the average domain length diverges as we increase the lattice size towards the thermodynamic limit. Therefore, as earlier anticipated, the phenomenon of magnetization reversal is a finite size effect relevant for the growth of magnetic films in confined geometries.

At this point it is useful to perform a comparison between the results obtained with the MEM and the well known behavior of the Ising model analyzing the interplay between broken symmetry and finite-size effects at thermal phase transitions. In ordinary thermally driven phase transitions, the system changes from a disordered state at high temperatures to a spontaneously ordered state at temperatures below some critical value T_c, where a second-order phase transition takes place. Regarding the equilibrium Ising model as the archetypical example, one concludes that, in the absence of an externally applied magnetic field $(H=0)$, the low temperature ordered phase is a state with nonvanishing spontaneous magnetization $(\pm M_{\rm sp}$, the sign depending on the initial state). This spontaneous symmetry breaking is possible in the thermodynamic limit only. In fact, it is found that the magnetization M of a finite sample formed by N particles, defined by

$$M(T,H=0)=\frac{1}{N}\sum_{i=1}^{N} S_i(T,H=0), \tag{4}$$

can pass with a finite probability from a value near $+M_{\rm sp}$ to another near $-M_{\rm sp}$, as well as in the opposite direction. Consequently, the magnetization of a finite system, averaged over a sufficiently large observation time, vanishes at every positive temperature, irrespective of the (finite) size of the sample. The equation $M(T,H=0)\approx 0$ holds if the observation time $t_{\rm obs}$ becomes larger than the ergodic time $t_{\rm erg}$, which is defined as the time needed to observe the system passing from $\pm M_{\rm sp}$ to $\mp M_{\rm sp}$. Increasing the size of the

sample the ergodic time increases too, such that in the thermodynamic limit ergodicity is broken due to the divergence of the ergodic time, yielding broken symmetry. Since Monte Carlo simulations are restricted to finite samples, the standard procedure to avoid the problems treated in the foregoing discussion is to consider the root mean square (or the absolute) magnetization as an appropriate order parameter.[23] Turning back to the MEM, we find that the phenomenon of magnetization reversal [as shown in Fig. 1(a)] causes the magnetization of the whole film to vanish at every nonzero temperature, provided that the film's length l_F (which plays the role of t_{obs}) is much larger than l_D (which plays the role of t_{erg}). Therefore, as in the case of the Ising model,[23] in order to overcome shortcomings derived from the finite-size nature of Monte Carlo simulations we have measured the mean absolute column magnetization, given by

$$|m(i,L,T)| = \frac{1}{L}\left|\sum_{j=1}^{L} S_{ij}\right|. \tag{5}$$

In the stripped geometry used in this work the bias introduced by the linear seed (a starting column made up entirely of up spins) can be studied in plots of $|m(i,L,T)|$ versus i. It is found that $|m(i;L,T)|$ exhibits a transient growing period with a characteristic length of order L, followed by the attainment of a stationary regime. In addition, using several randomly generated seeds we could also establish that the system evolves into a given stationary state independently of the seed employed. Thus, the spin-up linear seed can be used throughout without loss of generality. This behavior has been observed throughout the range of interest studied in the present work, i.e., $16 \leqslant L \leqslant 1024$ and $0.2 \leqslant T \leqslant \infty$. So, the influence exerted on the spin system by the seed can be easily recognized and eliminated from our results just by disregarding the first $l_{Tr} = N.L$ columns, with N ranging between 10 and 50. The given procedure of column averaging out from the transient region represents a significant advantage of the stripped geometry used for the simulation of the MEM, in addition to that already mentioned (see Sec. II). In fact, when a single seed at the center of the sample is used, the definition of the average magnetization of the whole cluster is strongly biased by the cluster's kernel orientation at the early stages of the growing process. Hence, it is very difficult in this case to disentangle the stationary regime from the transient region. Moreover, film growth on planar substrata has the advantage that it can be implemented experimentally, e.g., via vapor deposition in vacuum, chemical deposition, electrodeposition, etc.

The mean column magnetization given by Eq. (3) is a fluctuating quantity that can assume $L+1$ values. Then, for given values of both L and T, the probability distribution of the mean column magnetization $(P_L(m))$ can straightforwardly be evaluated, since it represents the normalized histogram of m taken over a sufficiently large number of columns in the stationary region.[24–26] In the thermodynamic limit (lattice size going to infinite) the probability distribution $(P_\infty(m))$ of the order parameter of an equilibrium system at criticality is universal (up to rescaling of the order parameter) and thus it contains very useful and interesting

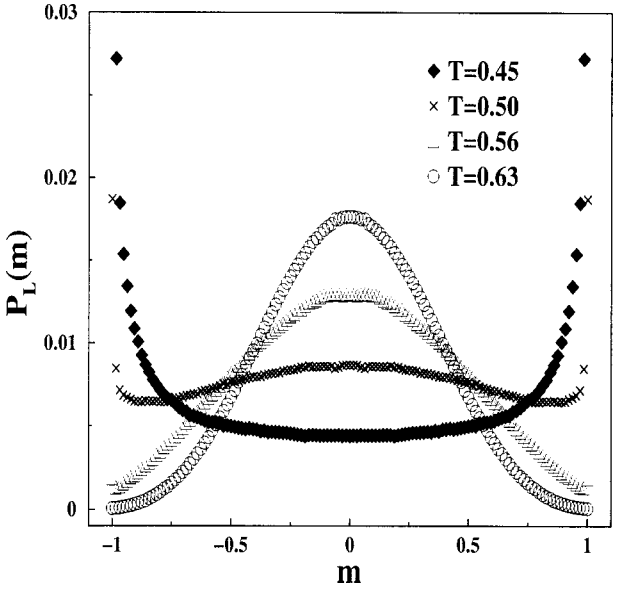

FIG. 4. Data corresponding to the $(1+1)$-dimensional MEM: plots of the probability distribution of the mean column magnetization $P_L(m)$ vs m for the fixed lattice width $L=128$ and different temperatures, as indicated in the figure. The sharp peaks at $m=\pm 1$ for $T=0.45$ have been truncated, in order to allow a detailed observation of the plots corresponding to higher temperatures. This behavior resembles that of the one-dimensional Ising model.

information on the universality class of the system.[27–29] For example, $P_L(m)$ contains information about all momenta of the order parameter m, including universal ratios such as the Binder cumulant.[27] Figure 4 shows the thermal dependence of $P_L(m)$ for a fixed lattice size ($L=128$ in the present example) as obtained for the $(1+1)$ dimensional MEM. We can observe that at high temperatures $P_L(m)$ is a Gaussian centered at $m=0$. As the temperature is lowered, the distribution broadens and develops two peaks at $m=1$ and $m=-1$. Further decreasing the temperature causes these peaks to become dominant while the distribution turns distinctly non-Gaussian, exhibiting a minimum just at $m=0$. It should be pointed out that the emergence of the maxima at $m=\pm 1$ is quite abrupt. This behavior reminds us of the order parameter probability distribution characteristic of the one dimensional Ising model. In fact, for the well studied d-dimensional Ising model,[26,30] we know that for $T>T_c$, $P_L(M)$[31] is a Gaussian centered at $M=0$, given by

$$P_L(M) \propto \exp\left(\frac{-M^2 L^d}{2T\chi}\right), \tag{6}$$

where the susceptibility χ is related to order parameter fluctuations by

$$\chi = \frac{L^d}{T}(\langle M^2\rangle - \langle M\rangle^2). \tag{7}$$

By decreasing the temperature the order parameter probability distribution broadens, it becomes non-Gaussian, and near T_c it splits into two peaks that become more separated the lower the temperature. For $T<T_c$ and linear dimensions L much larger than the correlation length ξ of order parameter fluctuations, one may approximate $P_L(M)$ near the peaks by a double-Gaussian distribution, i.e.,

$$P_L(M) \propto \exp\left(\frac{-(M-M_{sp})^2 L^d}{2T\chi}\right) + \exp\left(\frac{-(M+M_{sp})^2 L^d}{2T\chi}\right), \quad (8)$$

where M_{sp} is the spontaneous magnetization, while the susceptibility χ is now given by

$$\chi = \frac{L^d}{T}(\langle M^2\rangle - \langle |M|\rangle^2). \quad (9)$$

From Eq. (6) it turns out that the Gaussian squared width σ^2 associated with high temperature distributions is very close to the second moment of the order parameter, i.e.,

$$\sigma^2 \approx \langle M^2\rangle. \quad (10)$$

It should be noticed that this equation is a straightforward consequence of the Gaussian shape of the order parameter probability distribution and, thus, it holds for the MEM as well. From the well known one-dimensional exact solution for a chain of L spins[32] one can establish the relationship

$$\chi = \frac{1}{T}\exp(2/T), \quad (11)$$

then, Eqs. (7) and (11) lead us to

$$\langle M^2\rangle = \frac{1}{L}\exp(2/T) \quad (12)$$

(where it has been taken into account that $\langle M\rangle = 0$ due to finite-size effects, irrespective of temperature). From Eqs. (10) and (12) we can see that the high temperature Gaussian probability distribution broadens exponentially as T is lowered, until it develops delta-like peaks at $M = \pm 1$ as a consequence of a boundary effect on the widely extended distribution. It should be noted that for $d \geqslant 2$ this phenomenon is prevented by the finite critical temperature which splits the Gaussian, as implied by Eq. (8).

Figure 5 shows the thermal evolution of the probability distribution as obtained for the $(2+1)$-dimensional MEM, using a lattice of side $L = 16$. For high temperatures, the probability distribution corresponds to a Gaussian centered at $m'' = 0$. At lower temperatures we observe the onset of two maxima located at $m'' = \pm M_{sp}$ $(0 < M_{sp} < 1)$, which become sharper and approach $m'' = \pm 1$ as T is gradually decreased. These low-temperature probability distributions clearly reflect the occurrence of the magnetization reversal effect already discussed for the case of $(1+1)$-dimensional magnetic films.

Figure 6 shows the location of the maximum of the probability distribution as a function of temperature for both $(d+1)$-dimensional MEM models (with $d = 1,2$) where we consider only maxima located at $m, m'' \geqslant 0$, since the distributions are symmetric around $m = m'' = 0$. After inspection of Fig. 6, the different qualitative behaviors of both systems becomes apparent. In fact, while for the $d = 2$ case we observe a smooth transition from the $m''_{max} = 0$ value characteristic of high temperatures to nonzero m''_{max} values that correspond to lower temperatures, the curve obtained for $d = 1$ shows, in contrast, a Heaviside-like jump. The latter case

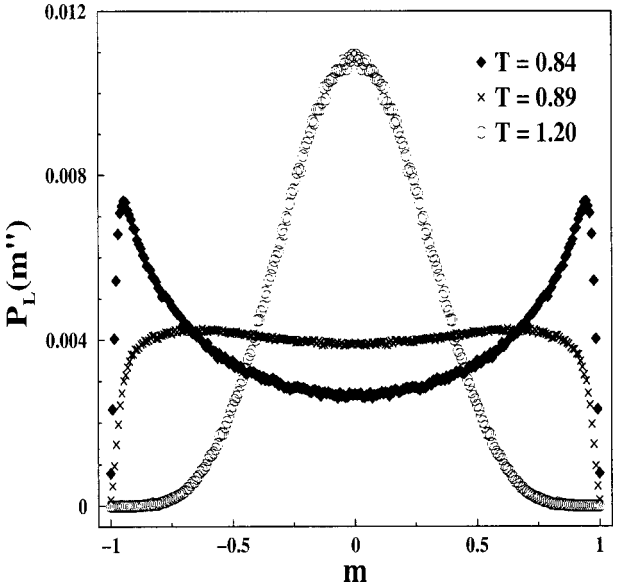

FIG. 5. Data corresponding to the $(2+1)$-dimensional MEM: plots of the probability distribution $P_L(m'')$ vs m'' for the fixed lattice size $L = 16$ and different temperatures, as indicated in the figure. The occurrence of two maxima located at $m'' = \pm M_{sp}$ (for a given value of M_{sp} such that $0 < M_{sp} < 1$) is the hallmark of a thermal continuous phase transition that takes place at a finite critical temperature.

reflects a behavior which is similar to that observed simulating the equilibrium Ising model in one-dimension. In order to carry out a quantitative comparison between both models, we have also evaluated the average absolute magnetization $(\langle |M_{Ising}|\rangle)$ for chains of the same length L as the columns of the $(1+1)$-dimensional MEM. Figure 7 shows log–linear plots of $\langle |M|_{Ising}\rangle(L,T) - \langle |m|_{MEM}\rangle(L,T)$ versus L^{-1} obtained for two different values of T. It becomes evident that

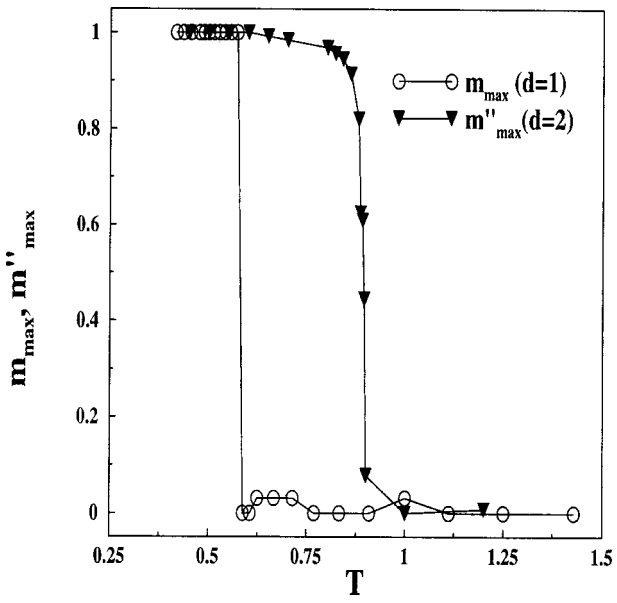

FIG. 6. Plots showing the location of the maximum of the probability distribution as a function of temperature for both $(d+1)$-dimensional MEM models $(d = 1,2)$. The lines are guides to the eye. The smooth transition for $d = 2$ constitutes more evidence of the nonzero critical temperature associated with the $(2+1)$ MEM.

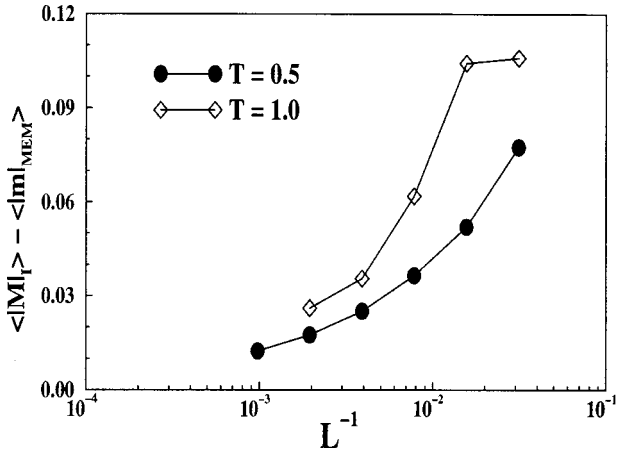

FIG. 7. Comparison of results corresponding to the $(1+1)$ MEM and the $d=1$ Ising model: log–linear plots of $\langle |M|_l \rangle (L,T) - \langle |m|_{\mathrm{MEM}} \rangle (L,T)$ vs L^{-1} for $T=0.5$ and $T=1.0$. The lines are guides to the eye. Hence, differences in the magnetization due to finite-size effects appear to vanish in the thermodynamic limit.

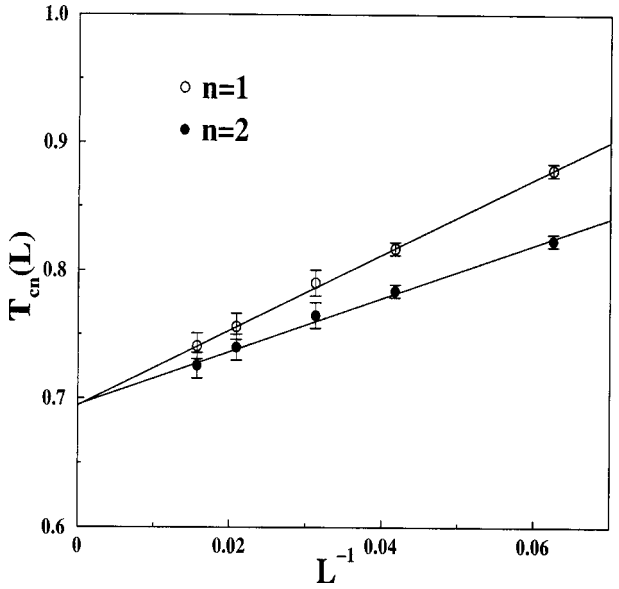

FIG. 8. Plots of the effective finite-size critical temperatures $T_{cn}(L)$ vs L^{-1} (for $n=1,2$) corresponding to the $(2+1)$-dimensional magnetic film. $T_{c1}(L)$ is defined as the value that corresponds to $\langle |m''| \rangle = 0.5$, while $T_{c2}(L)$ is the temperature that corresponds to the maximum of the susceptibility. The solid lines show the linear extrapolations that meet at the critical point given by $T_c = 0.69 \pm 0.01$.

the different L-dependent values of the magnetization are finite size effects observed as a consequence of the strips used. Such effects vanish in the thermodynamic limit.

In contrast to the $(1+1)$-dimensional case, the behavior exhibited by the $(2+1)$-dimensional MEM (e.g., as displayed by Figs. 5 and 6) is the signature of a thermal continuous phase transition that takes place at a finite critical temperature. It should be noted that this transition involves the entire system, that may be either in the disordered phase or in the ordered one, depending on temperature. The broken symmetry at a finite critical temperature T_c implied by the thermal continuous phase transition can be explained in terms of the broken ergodicity that occurs in the system when we tend to the thermodynamic limit $(L \to \infty)$ making use of the temperature dependence exhibited by the order parameter distribution function. In fact, if we introduce an ergodic length l_{erg} defined by $l_{\mathrm{erg}} \equiv l_D$, where l_D is the characteristic length of MEM's domains, we can carry out a complete analogy with the Ising model by associating l_{erg} to t_{erg} (the Ising model ergodic time) and the above mentioned film's total length l_F to the Ising model observation time t_{obs}. In this way, we encounter that excursions of m'' from $m''=+M_{\mathrm{sp}}$ to $m''=-M_{\mathrm{sp}}$ and *vice versa* occur at length scales on the order of l_{erg}. When the film's total length becomes larger and larger $(l_F \gg l_{\mathrm{erg}})$ the whole film's magnetization is averaged to zero. Furthermore, l_{erg} diverges as the strip's width becomes larger and larger, as shown in Fig. 3, and again broken symmetry arises as the consequence of broken ergodicity.

It should be noted that as in the case of equilibrium systems, in the present case various ''effective'' L-dependent critical temperatures can also be defined. In particular, we will define $T_{c1}(L)$ as the value that corresponds to $\langle |m''| \rangle = 0.5$ for fixed L, and $T_{c2}(L)$ as the temperature that corresponds to the maximum of the susceptibility for a given L, assuming that the susceptibility is related to order parameter fluctuations in the same manner as for equilibrium systems [as given by Eqs. (7) and (9)]. Then, we should be able to obtain T_c from plots of $T_{cn}(L)$ versus L^{-1} (for $n=1,2$), as it is shown in Fig. 8. Indeed, following this procedure we find that, for $L \to \infty$, both $T_{c1}(L)$ and $T_{c2}(L)$ extrapolate (approximately) to the same value, allowing us to evaluate the critical temperature $T_c = 0.69 \pm 0.01$ in the thermodynamic limit. Notice that T_c depends on both the coordination number and the topological structure of the lattice. Furthermore, these properties are not uniquely determined by the dimensionality. So, the small value of T_c obtained for the MEM, as compared to the Ising model on the square lattice with four nearest NNs given by $T_c^{I\mathrm{sing}} = 2.2692$,[32] reflects the fact that the effective number of occupied NN sites upon deposition of spins in the MEM ($\langle \mathrm{NN}_{\mathrm{MEM}} \rangle$) should be $\langle \mathrm{NN}_{\mathrm{MEM}} \rangle < 4$. Furthermore, the effective topological structure of the MEM compatible with the measured value of T_c remains an open question.

IV. CONCLUSIONS

In the present work we have studied the growth of magnetic films with ferromagnetic interactions between nearest neighbor spins in a $(d+1)$-dimensional rectangular geometry (for $d=1,2$), using Monte Carlo simulations. For both dimensions the phenomenon of spontaneous magnetization reversal is observed at low temperatures. Indeed, MEM films grown at low temperatures are constituted by a sequence of magnetic domains, each of them with a well defined magnetization, such that the magnetization of adjacent domains is antiparallel. Further increasing the temperature causes the onset of disorder in the bulk of the domains. Subsequently, a rounded effective transition to a fully disordered state takes place. These pseudo-''phase transitions'' occur at film width L dependent effective critical temperatures. However, in the thermodynamic limit $(L \to \infty)$, the $(1+1)$-dimensional

MEM is not critical (the transition takes place at $T=0$), while a true second-order phase transition is expected to occur at a finite temperature ($T_c=0.69\pm0.01$) in the $(2+1)$-MEM. The observed behavior is reminiscent of that of the equilibrium Ising model, although it should be stressed that the MEM is a far-from-equilibrium growing system.

The finite size of the films causing magnetization reversal and the occurrence of effective order–disorder transitions may be undesired effects that shall be avoided in the preparation of high quality magnetic films. However, these shortcomings may disappear if the film strongly interacts with the substrate where the actual growing process takes place. Further studies on the growth of magnetic films in the presence of surface magnetic films that account for the interaction with the substrate are under progress.[33,34]

ACKNOWLEDGMENTS

This work is supported financially by CONICET, UNLP, ANPCyT, Fundación Antorchas (Argentina), and the Volkswagen Foundation (Germany).

[1] J. Shen *et al.*, Phys. Rev. B **56**, 2340 (1997).
[2] J. Hauschild, U. Gradmann, and H. J. Elmers, Appl. Phys. Lett. **72**, 3211 (1998).
[3] C.-Y. Hong, H.-E. Horng, F. C. Kuo, S. Y. Yang, H. C. Yang, and J. M. Wu, Appl. Phys. Lett. **75**, 2196 (1999).
[4] J. Shen, A. K. Swan, and J. F. Wendelken, Appl. Phys. Lett. **75**, 2987 (1999).
[5] J.-S. Tsay and Y.-D. Yao, Appl. Phys. Lett. **74**, 1311 (1999).
[6] H. J. Elmers, J. Hauschild, and U. Gradmann, Phys. Rev. B **59**, 3688 (1999).
[7] O. Pietzsch, A. Kubetzka, M. Bode, and R. Wiesendanger, Phys. Rev. Lett. **84**, 5212 (2000).
[8] E. V. Albano, K. Binder, D. Heermann, and W. Paul, Surf. Sci. **223**, 151 (1989).
[9] D. P. Landau and K. Binder, J. Magn. Magn. Mater. **104**, 841 (1992).
[10] D. Karevski and M. Henkel, Phys. Rev. B **55**, 6429 (1997).
[11] J. T. Ou, F. Wangand, and D. L. Lin, Phys. Rev. E **56**, 2805 (1997).
[12] F. D. A. Aratão Reis, Phys. Rev. B **58**, 394 (1998); **62**, 6565 (2000).
[13] M. Ausloos, N. Vandewalle, and R. Cloots, Europhys. Lett. **24**, 629 (1993), N. Vandewalle and M. Ausloos, Phys. Rev. E **50**, R635 (1994).
[14] M. Eden, in *Symposium on Information Theory in Biology*, edited by H. P. Yockey (Pergamon, New York, 1958); *Proceedings of the Fourth Berkeley Symposium on Mathematics, Statistics and Probability*, edited by F. Neyman (University of California Press, Berkeley, 1961), Vol. IV, p. 223.
[15] A. L. Barabasi and H. E. Stanley, *Fractal Concepts in Surface Growth* (Cambridge University Press, New York, 1995).
[16] *Fractals and Disordered Media*, edited by A. Bunde and S. Havlin (Springer, Heidelberg, 1991).
[17] Y. V. Ivanenko, N. I. Lebovka, and N. V. Vygornitskii, Eur. Phys. J. B **11**, 469 (1999).
[18] E. Ising, Z. Phys. **31**, 253 (1925).
[19] U. Bovensiepen *et al.*, Phys. Rev. Lett. **81**, 2368 (1998).
[20] B. M. McCoy and T. T. Wu, *The two dimensional Ising model* (Harvard University Press, Cambridge, MA, 1973).
[21] T. Ono, H. Miyajima, K. Shigeto, and T. Shinjo, Appl. Phys. Lett. **72**, 1116 (1998).
[22] T. Aign *et al.*, Phys. Rev. Lett. **81**, 5656 (1998).
[23] K. Binder and D. W. Heermann, in *Monte Carlo Simulation in Statistical Physics*, Springer Series in Solid State Sciences 80 (Springer, Berlin, 1992).
[24] K. Binder and D. Stauffer, "A simple introduction to Monte Carlo simulation and some specialized topics," in *Applications of the Monte Carlo Method in Statistical Physics*, 2nd ed., edited by K. Binder (Springer, Berlin, 1987).
[25] K. Binder, *Encyclopedia of Applied Physics* (VCH, Heidelberg, 1994), Vol. 10, p. 567.
[26] K. Binder, in *Conference Proceedings Vol. 49, Monte Carlo and Molecular Dynamics of Condensed Matter Systems*, edited by K. Binder and G. Ciccotti (SIF, Bologna, 1996), Vol. 49, Chap. 5, p. 124.
[27] K. Binder, Z. Phys. B: Condens. Matter **43**, 119 (1981).
[28] A. D. Bruce, J. Phys. C **14**, 3667 (1981).
[29] M. M. Tsypin and H. W. J. Blöte, Phys. Rev. E **62**, 73 (2000).
[30] L. D. Landau and E. M. Lifshitz, *Statistical Physics*, 3rd ed. (Pergamon, Oxford, 1980), Part 1.
[31] Notice that according to the definitions given by Eqs. (3) and (4) we have used $P_L(m)$ and $P_L(M)$ for the MEM and the Ising model, respectively.
[32] R. J. Baxter, *Exactly Solved Models in Statistical Mechanics* (Academic, New York, 1982).
[33] J. Candia and E. V. Albano, Eur. Phys. J. B **16**, 531 (2000).
[34] J. Candia and E. V. Albano (unpublished).